Supporting Information

Tuning the Mechanical Properties of Metallopolymers via Ligand Interactions: A Combined Experimental and Theoretical Study

Yuval Vidavsky,[†,‖] Michael R. Buche,[†,‖] Zachary M. Sparrow,[‡] Xinyue Zhang,[§] Steven J. Yang,[†] Robert A. DiStasio Jr.,[‡,*] and Meredith N. Silberstein[†,*]

[†]Sibley School of Mechanical and Aerospace Engineering, [‡]Department of Chemistry and Chemical Biology, Baker Laboratory, and [§]Department of Materials Science and Engineering, Cornell University, Ithaca, New York 14853, United States.

[‖]Y.V. and M.R.B. contributed equally to this work

Table of Contents

General 2

Polymer Synthesis 2

Dog-Bone Mold Preparation 4

Tensile Test Methods 4

Glass Transition Temperature Determination 5

Theoretical Backbone Stiffness 6

Cyclic Stress-Strain Response Compared to Monotonic Loading 7

Computational Details 8

Dynamic Mechanical Analysis for Ni-nIm Materials 13

IR Spectra and Color of Ni-nIm and Ni-2Ligand Materials 14

References 16

General

Unless otherwise noted, solvents and reagents were purchased and used without further purification. Nickel(II) acetate tetra hydrate, imidazole, 2-methyimidazole, and dimethylamine 2M in THF were purchased from Oakwood Chemical. Piperidine, pyridine, 2-carboxyethyl acrylate, Diphenyl(2,4,6-trimethylbenzoyl)phosphine oxide, and 2-Hydroxy-2-methylpropiophenone were purchased from Millipore-Sigma. 2-Hydroxyethyl acrylate was purchased from TCI America. Sylgard^{TM} 184 was purchased from Electron Microscopy Sciences. Infrared (IR) spectra were recorded in the range of 600 – 4000 cm^{-1} with 8 cm^{-1} resolution on a Bruker Vertex V80V Vacuum FTIR system in ATR mode under vacuum.

Polymer Synthesis

Preparation of the acrylic formulation with Ni^{2+} crosslinker: A solution of nickel acetate tetra hydrate (34.9 gr, 140 mmol) in methanol (200 ml) was added to a mixture of 2-hydroxyethyl acrylate (246.7 gr, 2.124 mol) and 2-carboxyethyl acrylate (40.4 gr, 280 mmol). The acetic acid was distilled out under reduced pressure (50 mmhg) at 65 °C. The formulation was stored in the dark at 4 °C and was used for the preparation of all the nickel crosslinked materials.

General procedure for neutral ligand attachment: The appropriate ligand in the indicated number of equivalents was added slowly to the Ni^{2+} acrylic formulation at 0 °C while stirring. The modified nickel formulation was cured according to the general UV curing procedure and was tested 24 h after preparation.

General procedure for UV free radical polymerization: Diphenyl(2,4,6-trimethylbenzoyl)phosphine oxide (0.005 eq for every acrylic group) and 2-hydroxy-2-methylpropiophenone (0.017 eq for every acrylic group) were added to the acrylic formulation.

The UV curable formulation was transferred to a dog-bone shaped silicone mold (Figure S1) pressed between two glass plates laminated with scotch tape (to prevent adhesion of the cured polymer to the glass). The formulation was cured by 365 nm UV light irradiation generated by two lamps (6 Watt 365 nm, VWR) for 45 minutes.

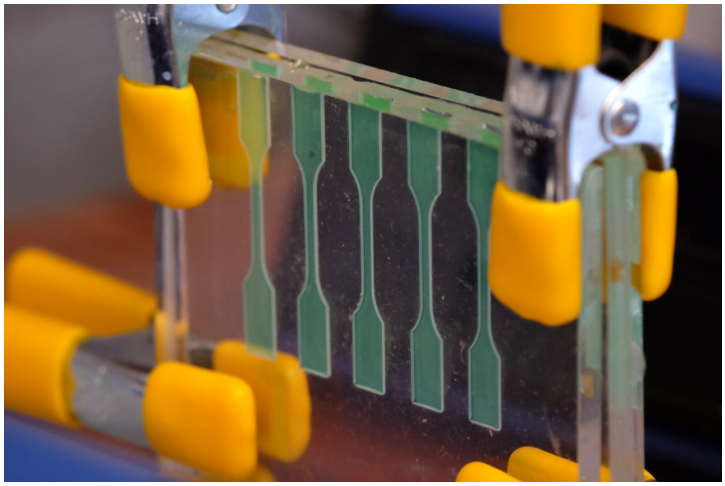

Figure S1. Polymerization setup, made from dog-bone silicone mold pressed between two laminated glass plates.

Preparation of the linear polymer, poly(2-hydroxyethyl acrylate-co-2-carboxyethyl acrylate): A mixture of 2-hydroxyethyl acrylate (6.15 gr, 53.0 mmol) and 2-carboxyethyl acrylate (1.01 gr, 7.0 mmol) was pretreated under reduced pressure (50 mm Hg) at 65 °C to mimic the same preparation conditions as the nickel crosslinked materials. The formulation was cured according to the general UV curing procedure and was tested 24 h after preparation.

Preparation of the linear polymer poly(2-hydroxyethyl acrylate) with dispersion of $Ni(OAc)_2(H_2O)_4$: A solution of nickel acetate tetra hydrate (1.40 gr, 5.6 mmol) in methanol (10 ml) was added to 2-hydroxyethyl acrylate (9.87 gr, 85 mmol). The methanol was removed under reduced pressure (50 mmhg) at 65 °C. The formulation was cured according to the general UV curing procedure and was tested 24 h after preparation.

Preparation of the linear polymer poly(2-hydroxyethyl acrylate): 2-hydroxyethyl acrylate (9.87 gr, 85 mmol) was pretreated under reduced pressure (50 mm Hg) at 65 °C to mimic the same preparation conditions as the nickel crosslinked materials. The formulation was cured according to the general UV curing procedure and was tested 24 h after preparation.

Dog-Bone Mold Preparation

First, an acrylic mold was prepared. Five dog-bones (Figure S2) matching the desire final specimen shape were laser cut from 1.5 mm thick PMMA panel. The acrylic dog-bones were solvent welded to an acrylic plate with 5.5 mm separation between dog-bones in the acrylic mold. A silicone mold was then prepared by casting two parts PDMS resin (SYLGARD™ 184) onto the acrylic mold. The resin was cured for 48 h at room temperature and an additional 5 h at 70 °C. The silicone molds were sprayed with EASE RELEASE™ 200 (Smooth On Inc.) before each use.

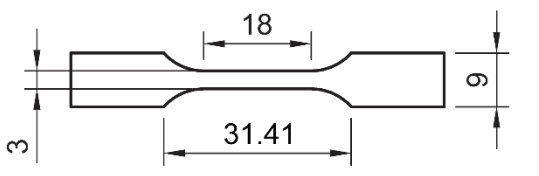

Figure S2. Dog-bone dimensions in mm.

Tensile Test Methods

Tensile tests were performed on a Zwick-Roell Z010 system with a 500 N capacity load cell (X-Force HP, Zwick-Roell). Constant strain rate, cyclic, and stress relaxation tests were performed with displacement control using engineering strain rates and assuming an effective gage length of 28.00 mm. Both the cyclic and stress relaxation tests were conducted at an engineering strain rate of 0.114 s^{-1}. For the cyclic test, the change in crosshead direction is specified by displacement when loaded and by force (0.1 N) when unloaded.

Stress and strain were calculated from force and extension recorded during tensile tests. Engineering strain is given by $\varepsilon_{eng} = \Delta L/L_0$, where L_0 is the initial gage length obtained by linear finite element simulation of the tensile specimen geometry. True stress is given by $\sigma_{eng} = F/A_0$ where F is the recorded force and A_0 is the original specimen cross-sectional area. Elastic moduli were determined by a linear fit to the stress-strain curve over the initial linear region. Yield stresses were determined by determining the point on the stress strain curve directly below the point of intersection between the line tangent to the initial linear region and the line tangent to the linear region immediately following the yield peak.

Glass Transition Temperature Determination

Glass transition temperatures (T_g) of the samples were measured by Dynamic Mechanical Analysis (DMA) Q800 (TA Instruments) with a film tension clamp under nitrogen atmosphere. The preload force was 0.01 N, and an oscillation strain 0.1% was performed on the sample with a frequency of 1Hz. The sample was equilibrated at -30 °C for 2 mins and then heated up to 150 °C with speed 3 °C/min.

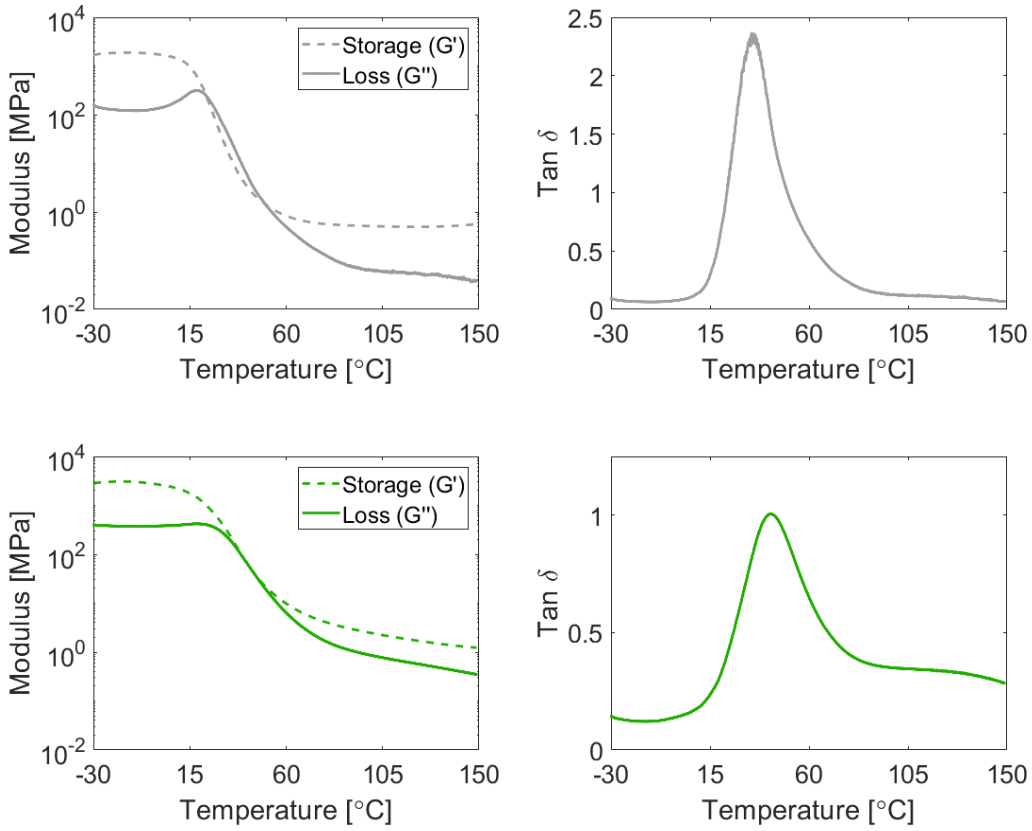

Figure S3. Storage and loss modulus (left) and tan δ (right) for **Linear** (top) and **Ni (**bottom).

Theoretical Backbone Stiffness

The backbone stiffness between crosslinks was estimated by performing a molecular dynamics (MD) simulation of seven repeat units of poly(2-hydroxyethyl acrylate). All MD simulations were performed using the large-scale atomic/molecular massively parallel simulator (LAMMPS)[1] on the Extreme Science and Engineering Discovery Environment *Stampede2* cluster.[2] A CVFF force field was used to define the interactions between the atoms in the polymer chain.[3] The chain was first equilibrated using Langevin dynamics for 0.1 ns (with a time step of 1.0 fs) at 500 K in the *NVE* ensemble and 0.1 ns (with a time step of 0.5 fs) at 500 K and atmospheric pressure in the *NpT* ensemble. This was followed by cooling the system at a constant rate from 500 K to 300 K over 0.25 ns (with a time step of 0.5 fs) in the *NpT* ensemble, followed by a 1.0 ns simulation (with a

timestep of 0.5 fs) at 300 K and atmospheric pressure in the *NpT* ensemble. The polymer chain was then deformed for 1.0 ns (with a time step of 1.0 fs) in the *NVE* ensemble by fixing the carbon at one end of the chain and pulling on the carbon at the other end of the chain along the radial vector between them at a controlled force rate of 20.8 nN/ns. Langevin dynamics were used during the pulling step to maintain the temperature at 300 K.

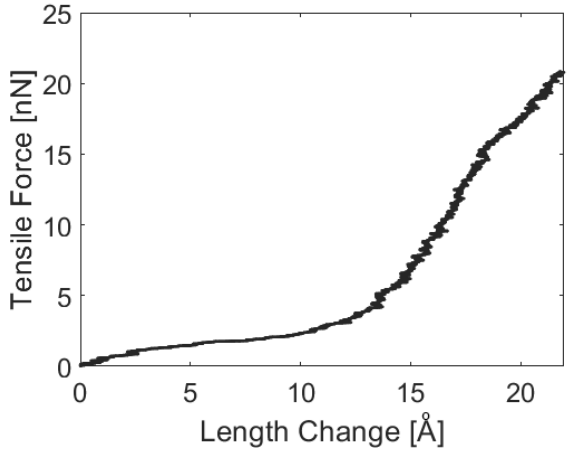

Figure S4. Theoretically (MD) obtained mechanical response in the average length of backbone between crosslinks from which the initial stiffnesses is approximately 0.4 nN/Å and the maximum tangent stiffness is approximately 2.4 nN/Å.

Cyclic Stress-Strain Response Compared to Monotonic Loading

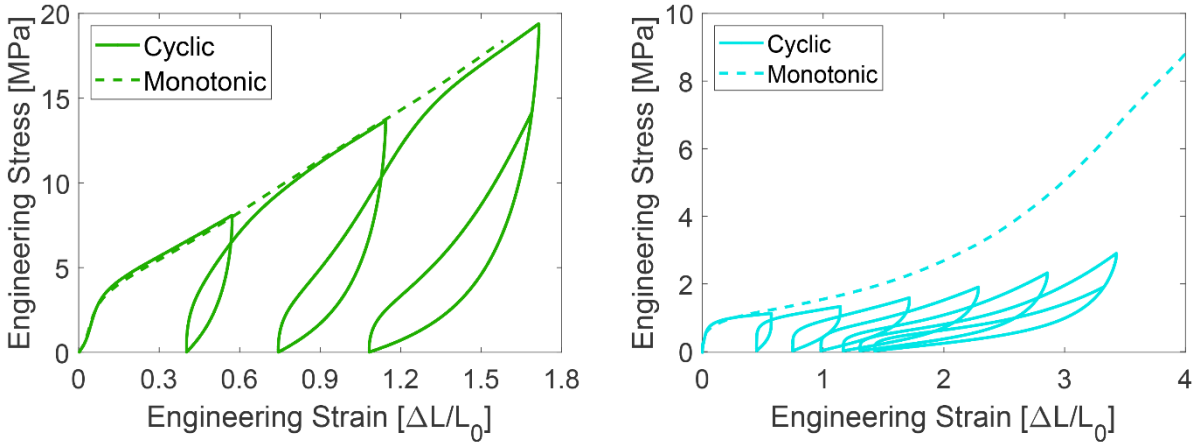

Figure S5. Cyclic and monotonic response for **Ni** (left) and **Ni-2Im** (right).

Computational Details

All calculations were carried out using the Extreme Science and Engineering Discovery Environment (XSEDE) *Stampede2* cluster[2] and the U.S. Department of Defense High Performance Computing Modernization Program (HPCMP) *Mustang* and *Centennial* clusters.

Geometry Optimizations of the Model Systems: All calculations were performed with the Q-Chem software package[4] (5.1 development version) using the ωB97X-V[5] density functional approximation and the def2-TZVPP[6] basis set. All SCF calculations were converged with a tight DIIS convergence threshold (`SCF_CONVERGENCE = 10^-9`) and integral threshold of (`THRESH = 10^-14`) unless otherwise noted. Symmetry was ignored during all calculations (`SYMMETRY = FALSE`, `SYM_IGNORE = TRUE`), and the force, displacement, and energy convergence criteria were set to their minimum respective values (`GEOM_OPT_TOL_GRADIENT = 1`, `GEOM_OPT_TOL_DISPLACEMENT = 1`, `GEOM_OPT_TOL_ENERGY = 1`). Various nickel-ligand conformations and ligand rotations were sampled as starting points for geometry optimizations to ensure convergence to the global energy minimum of each nickel crosslink structure. In addition, numerous starting points for the second coordination sphere molecules were sampled (when appropriate) to obtain the lowest energy configurations. All calculations treated the electronic wavefunction as a high-spin triplet; for all imidazole containing compounds, we computed the corresponding singlet-triplet gaps to confirm a triplet ground state. During all calculations, the spin contamination of the wavefunction was minimal with $\langle S^2 \rangle$ values ranging from 2.0029 to 2.0043. Subsequent harmonic vibrational frequency analyses (using a numerical finite-difference scheme with `FDIFF_STEPSIZE = 100`) were performed to confirm that all optimized geometries were minima with no imaginary frequencies.

Applying External Forces to the Crosslink: The mechanical responses of the structures were then investigated by applying equal and opposite forces at the outer methyl carbon atoms using the External Force Explicitly Included (EFEI)[7] algorithm. The external force was incrementally increased in steps of 0.1 nN, and the geometry was reoptimized (as described above) until one of the nickel-carboxylate bonds ruptures and the complex dissociates from the applied forces. This rupturing event was defined as a failure in the geometry optimization procedure to converge after a total of 750 iterations.

Free Energy Barriers: The dissociated structures from the EFEI algorithm (i.e., the geometries at the point of rupture) were taken as starting points in subsequent force-free geometry optimizations to obtain the optimized configurations for each ruptured crosslink (as described above). To compute the corresponding free-energy barriers, the frozen string method (FSM)[8,9] was employed to compute an approximate reaction pathway connecting the (force-free) optimized intact and ruptured structures. Subsequent transition state (TS) searches were performed on the maximum-energy configurations from the FSM pathways using the same force, displacement, and energy convergence criteria as above, and a maximum allowed step size of 0.05 (`GEOM_OPT_DMAX = 50`). Depending on the difficulty associated with finding the final TS, FSM calculations used 20-55 nodes and 6-20 orthogonal gradients. All TS structures were verified to have a single imaginary frequency (which connected the corresponding reactant and product) using the numerical Hessian procedure described above. Thermal contributions to the free energy were computed at a temperature of 298.15 K and a pressure of 1 atm using partition functions derived from the standard ideal gas (IG) and rigid rotor-harmonic oscillator (RRHO) approximations.

Consecutive Ligand Binding Energies: The geometries used for computing consecutive binding free energies were optimized according to the procedure described above, based on starting configurations generated by systematically replacing each of the four water molecules initially bound to the nickel center with an imidazole ligand (see Figure S6). The replaced water molecules were taken to be infinitely separated from the complex (and not included in the second coordination sphere), which is needed to maintain size consistency in the binding free energies. Binding free energies for the consecutive addition of n ligands were then computed according to:

$$\Delta G_{\mathrm{bind}}[n] = \left(G[\mathrm{Ni(OAc)_2L}_n\mathrm{(H_2O)}_{4-n}] + G[\mathrm{H_2O}]\right) - \left(G\left[\mathrm{Ni(OAc)_2L}_{n-1}\mathrm{(H_2O)}_{4-(n-1)}\right] + G[\mathrm{L}]\right),$$

where $G[X]$ is the free energy of the X species, and n = 1, 2, 3, 4 is the number of coordinating ligands. The results are reported in Table S1 for the imidazole (Im), methylimidazole (MeIm), pyridine (Py), piperidine (Pipe), and dimethylamine (DMA) ligands.

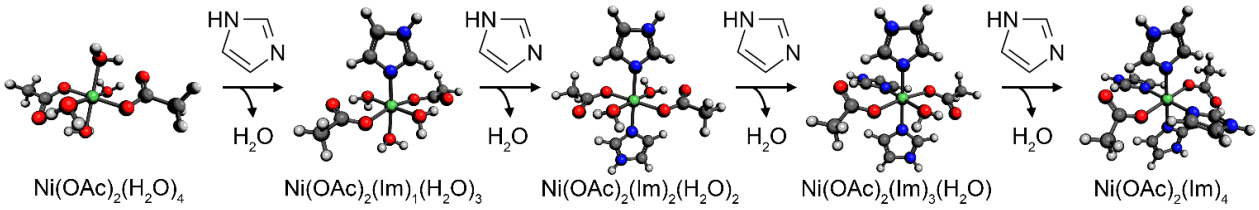

Figure S6. Illustration of the procedure used to calculate the theoretical binding free energies for the consecutive addition of n = 1, 2, 3, 4 imidazole ligands.

Table S1. Theoretical binding free energies (in kcal/mol) for the consecutive addition of a given ligand to the nickel center.

Ligand	$\Delta G_{\mathrm{bind}}[1]$	$\Delta G_{\mathrm{bind}}[2]$	$\Delta G_{\mathrm{bind}}[3]$	$\Delta G_{\mathrm{bind}}[4]$
Im	-4.60	-8.34	-0.80	0.53
MeIm	-5.15	-9.28	-0.64	-
Py	-4.79	-3.99	1.45	-
Pipe	-7.78	-6.83	0.87	-
DMA	-6.19	-5.57	1.23	-

Population Analysis: To determine the number of imidazole ligands (Im) bound to each Ni center at equilibrium, we considered a finite system consisting of N metal centers (representing a polymer with N non-interacting nickel-carboxylate crosslinks). Each of these metal centers was taken to have the following molecular formula, $Ni(OAc)_2L_n(H_2O)_{4-n}$, and was allowed to reside in one of five states, ranging from no bound Im ligands (n = 0) to four bound Im ligands (n = 4). The corresponding free energies of each state (relative to the n = 0 state for which $\Delta G[0]$ was set to 0.0 kcal/mol) were taken as the sum of the consecutive binding free energies in Table S1, i.e., $\Delta G[n] = \Sigma_k \Delta G_{bind}[k]$ for $1 \leq k \leq n$. With these $\Delta G[n]$ values in hand, we enumerated all possible energy levels for a system containing N metal centers, ranging from all metal centers in the n = 0 state to all metal centers in the n = 4 state. Enumerating energy *levels* (instead of explicitly enumerating system *states*) enables us to simulate larger system sizes by dramatically decreasing the computational effort associated with the enumeration. To construct Fig. 3(a) in the manuscript, we considered m = 0 to 5 equivalents of Im (in increments of 0.125). For a given m, we selected all of the enumerated levels which contain less than mN Im ligands for the analysis described below. Here we note that each energy level corresponds to all of the system states within the same permutation group. In other words, the degeneracy of each energy level arises from the permutational symmetry of the system, in which one can swap the states of any two Ni centers without changing the total system energy. To calculate the degeneracy of the i-th energy level, g_i, we compute the number of distinct permutations via

$$g_i = \frac{N!}{N_{i,0}!\, N_{i,1}!\, N_{i,2}!\, N_{i,3}!\, N_{i,4}!},$$

in which $N_{i,n}$ denotes the number of Ni centers bound to n Im ligands. It follows that the probability of occupying the i-th energy level, P_i, is given by:

$$P_i = \frac{g_i \exp\left[\frac{-\Delta G_i}{k_B T}\right]}{Q},$$

in which k_B is the Boltzmann constant, T is the temperature, and Q is the canonical partition function,

$$Q = \sum_i g_i \exp\left[\frac{-\Delta G_i}{k_B T}\right].$$

In both of these expressions, we note that the total energy of the i-th energy level is given by:

$$\Delta G_i = \sum_n N_{i,n} \Delta G[n].$$

With P_i in hand, the probability of occupying the n-th Ni state, π_n, can then be computed as follows:

$$\pi_n = \frac{1}{N} \sum_i N_{i,n} P_i,$$

in which the sum over i includes all energy levels that are possible when m equivalents of Im ligands are added to the system. In this work, we considered $N = 48$ Ni centers and $T = 298.15$ K, which yields π_n values that are converged to within ~1%. As such, the error made with this finite ensemble is negligible when compared to the uncertainties in the computed $\Delta G[n]$ values.

Dynamic Mechanical Analysis for Ni-nIm Materials

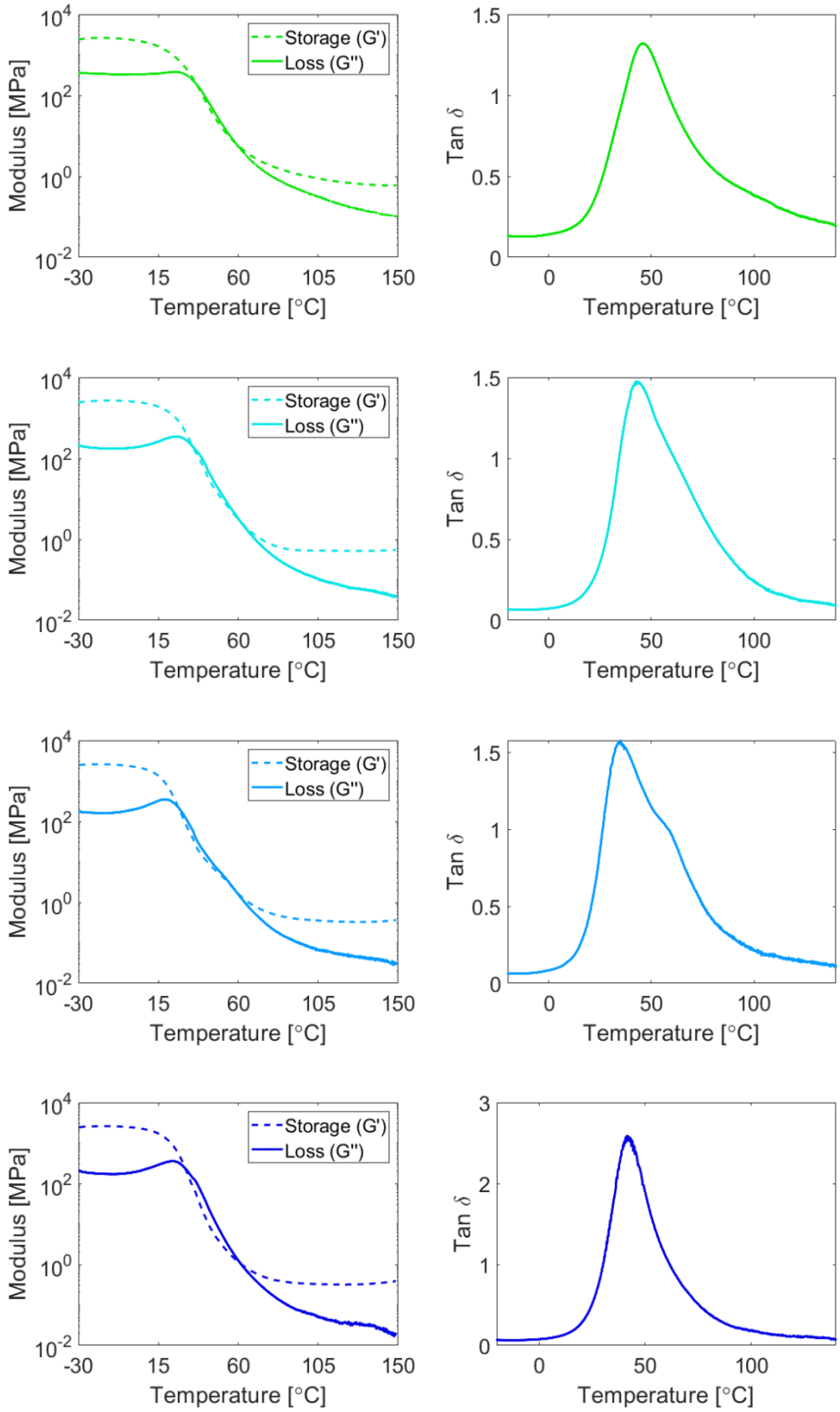

Figure S7. Storage and loss modulus (left) and tan δ (right) for **Ni-1Im**, **Ni-2Im**, **Ni-3Im**, **Ni-4Im**, from top to bottom.

IR Spectra and Color of Ni-nIm and Ni-2Ligand Materials

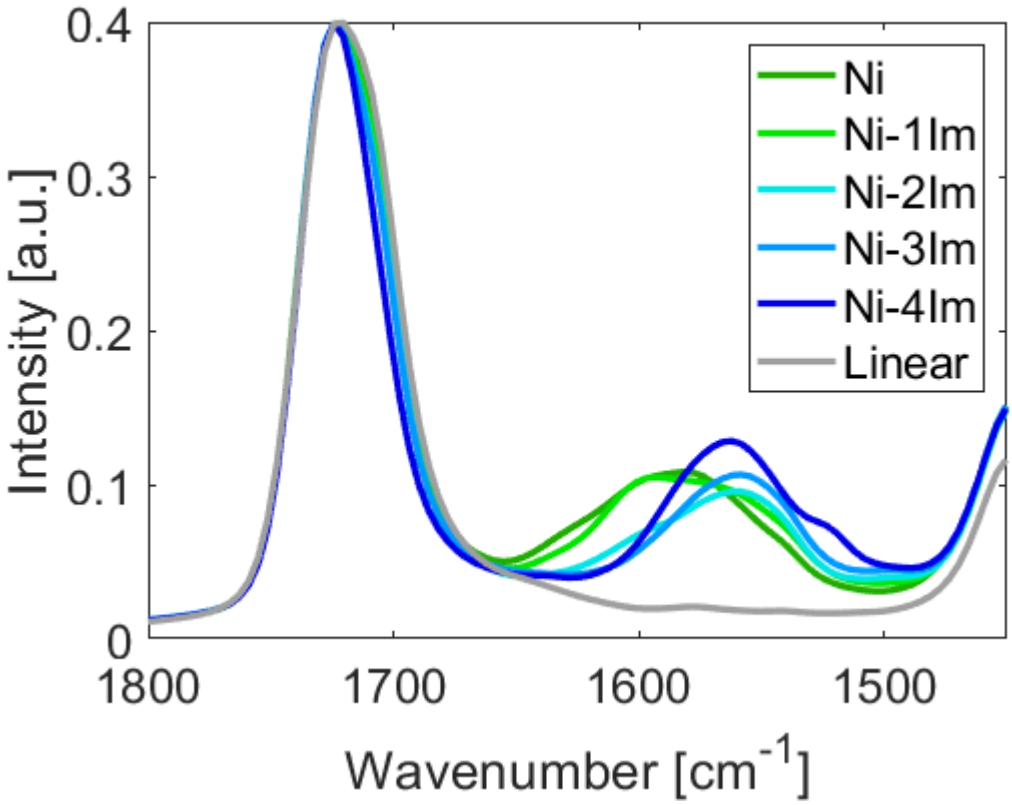

Figure S8. IR spectra of polymers with different numbers of Im equivalents per Ni center.

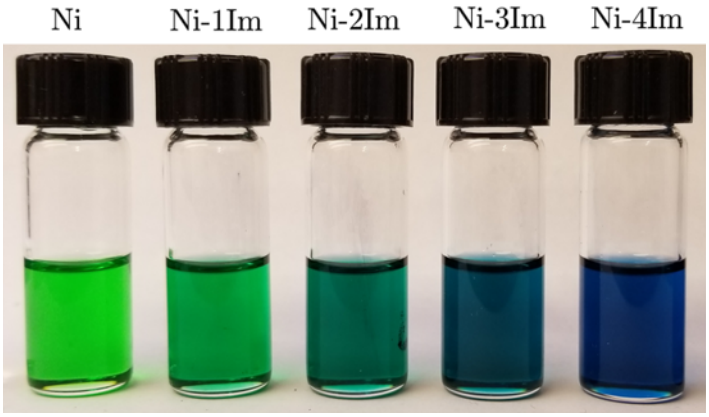

Figure S9. Nickel carboxylate crosslinkers in solution with increasing amounts of imidazole. All solutions were prepared according to the general procedure for neutral ligand attachment (see above).

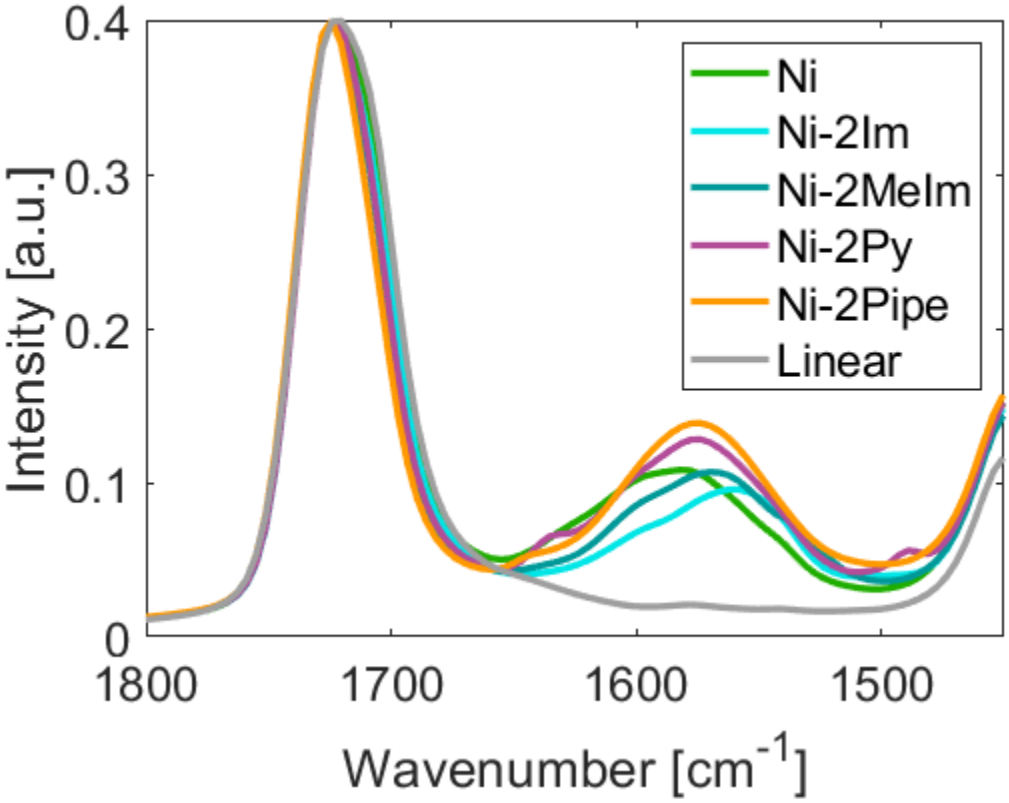

Figure S10. IR spectra of polymers with different types of ligands.

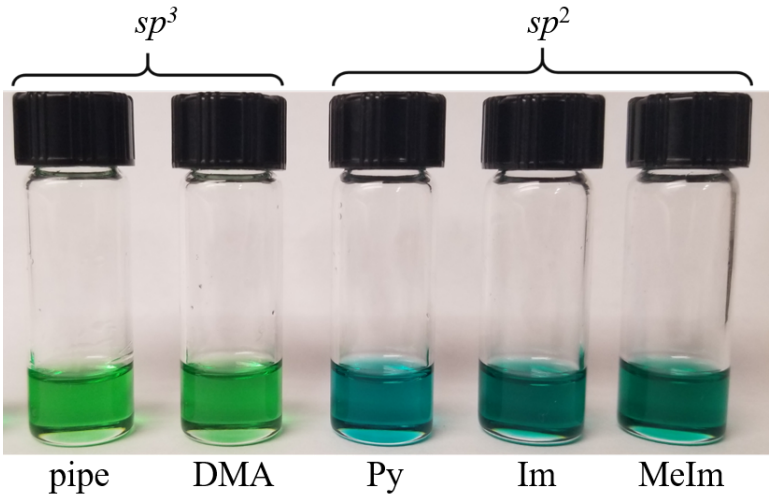

Figure S11. Differences in color for solutions of **Ni-2Pipe** and **Ni-2DMA** (sp^3 nitrogen) *vs*. **Ni-2Py**, **Ni-Im** and **Ni-2MeIm** (sp^2 nitrogen). All solutions were prepared according to the general procedure for neutral ligand attachment (see above).

References

(1) Plimpton, S. Fast Parallel Algorithms for Short-Range Molecular Dynamics. *J. Comput. Phys.* **1995**, 117, 1-19

(2) Towns, J. W.; Cockerill, T; Dahan, M; Foster, I.; Gaither, K.; Grimshaw, A.; Hazlewood, V.; Lathrop, S.; Lifka, D.; Peterson, G. D.; Roskies, R. XSEDE: Accelerating Scientific Discovery. *Comput. Sci. Eng*. **2014**, 16, 62.

(3) Dauber-Osguthorpe, P. Roberts, V.A. Osguthorpe, D. J., Wolff, J., Genest, M., & Hagler, A. T. Structure and energetics of ligand binding to proteins: Escherichia coli dihydrofolate reductase-trimethoprim, a drug-receptor system. *Proteins: Structure, Function, and Bioinformatics*, **1988**, 4 (1), 31-47

(4) Shao, Y.; Gan, Z.; Epifanovsky, E.; Gilbert, A. T. B.; Wormit, M.; Kussmann, J.; Lange, A. Behn, A.; Deng, J.; Feng, X.; Ghosh, D.; Goldey, M.; Horn, P. R.; Jacobson, L. D.; Kaliman, I.; Khaliullin, R. Z.; Kus, T.; Landau, A.; Liu, J.; et al. Advances in Molecular Quantum

Chemistry Contained in the Q-Chem 4 Program Package. *Mol. Phys.* **2015**, *113* (2), 184–215.

(5) Mardirossian, N.; Head-Gordon, M. ωB97X-V: A 10-Parameter, Range-Separated Hybrid, Generalized Gradient Approximation Density Functional with Nonlocal Correlation, Designed by a Survival-of-the-Fittest Strategy. *Phys. Chem. Chem. Phys.* **2014**, *16* (21), 9904–9924.

(6) Weigend, F.; Ahlrichs, R. Balanced Basis Sets of Split Valence, Triple Zeta Valence and Quadruple Zeta Valence Quality for H to Rn: Design and Assessment of Accuracy. *Phys. Chem. Chem. Phys.* **2005**, *7* (18), 3297–3305.

(7) Ribas-Arino, J.; Shiga, M.; Marx, D. Understanding Covalent Mechanochemistry. *Angew. Chem. Int. Ed.* **2009**, *48* (23), 4190–4193.

(8) Behn, A.; Zimmerman, P. M.; Bell, A. T.; Head-Gordon, M. Efficient Exploration of Reaction Paths via a Freezing String Method. *J. Chem. Phys.* **2011**, *135* (22), 224108.

(9) Mallikarjun Sharada, S.; Zimmerman, P. M.; Bell, A. T.; Head-Gordon, M. Automated Transition State Searches without Evaluating the Hessian. *J. Chem. Theory Comput.* **2012**, *8* (12), 5166–5174.